MADPH-07-1488
HRI-P-07-05-001

Pair Production of Doubly-Charged Scalars: Neutrino Mass Constraints and Signals at the LHC

Tao Han [a,d],* Biswarup Mukhopadhyaya [b],† Zongguo Si [c],‡ and Kai Wang [a§]

[a] *Department of Physics, University of Wisconsin, Madison, WI 53706, USA*

[b] *Harish-Chandra Research Institute, Allahabad 211019, INDIA*

[c] *Department of Physics, Shandong University, Jinan, Shandong 250100, P.R. China*

[d] *Center for High Energy Physics, Tsinghua University, Beijing 100084, P.R. China*

We study the pair production of doubly charged Higgs bosons at the Large Hadron Collider (LHC), assuming the doubly charged Higgs to be part of an $SU(2)_L$ triplet which generates Majorana masses for left-handed neutrinos. Such pair-production has the advantage that it is not constrained by the triplet vacuum expectation value, which tends to make the single production rate rather small. We point out that, in addition to the Drell-Yan (DY) production mechanism, two-photon processes also contribute to $H^{++}H^{--}$ production at a level comparable to the QCD corrections to the DY channel. Decays of the doubly charged Higgs into both the $\ell^+\ell^+$ and W^+W^+ modes are studied in detail to optimize the signal observation over the backgrounds. Doubly charged scalars should be observable at the LHC with 300 fb^{-1} integrated luminosity in the $\ell^\pm\ell^\pm$ channel upto the mass range of 1 TeV even with a branching fraction of about 60%, and in the $W^\pm W^\pm$ channel upto a mass of 700 GeV. Such a doubly charged Higgs, if it is a member of a triplet generating neutrino masses, cannot be long-lived on the scale of collider detectors although it might lead to a displaced secondary vertex during its decay if it is lighter than about 250 GeV.

*Electronic address: than@hep.wisc.edu

†Electronic address: biswarup@mri.ernet.in

I. INTRODUCTION

Higgs bosons in representations of $\mathrm{SU}(2)_L$ other than doublets occur in many extensions of the standard model. Among these, situations of special interest are created by $\mathrm{SU}(2)_L$ triplet scalars which occur in various scenarios, ranging from left-right symmetric models to Little Higgs theories [1, 2, 3, 4]. Complex scalar triplets with a hypercharge $Y = 2$ are particularly rich in this context in terms of their phenomenological implications. Once we allow lepton number violation by two units, the complex triplet can couple to left-handed leptons in a gauge-invariant and renormalizable manner and give rise to Majorana masses for neutrinos. No right-handed neutrinos need to be postulated in such a scenario. At the same time, the complex triplet contains a doubly charged component (H^{++}), and the same $\Delta L = 2$ interactions with charged leptons open up a very spectacular set of decay channels for this state, namely, resonant decays into a pair of like-sign leptons. These channels not only lead to remarkably background-free signatures of the doubly charged scalars, but also demonstrate a crucial link between observations at high energy colliders and the widely discussed mechanism of neutrino mass generation. We explore such a link in this paper, in the context of the Large Hadron Collider (LHC).

Although the general idea is simple here and has been discussed earlier in different connections, including direct experimental searches at the Fermilab Tevatron [5, 6, 7], a number of subtle and challenging issues invariably come up in such a study, and we have done our best to address them.

First of all, the presence of a $Y = 2$ triplet $H = (H^{++}, H^+, H^0)$ allows the following $\Delta L = 2$ interaction with left-handed lepton doublets [8, 9]:

$$\mathcal{L} = Y^{ij}_{\ell\ell} L_i^T \; H \; C^{-1} L_j + \text{h.c.} \tag{1}$$

where C is the charge conjugation operator. In general, the triplet can develop a vacuum expectation value (vev, v'). It thus contributes to $\Delta L = 2$ Majorana masses for the neutrinos, proportional to $Y_{\ell\ell} v'$. The current observations from the neutrino oscillation experiments and cosmological bounds yield [10]

$$m_\nu = Y_{\ell\ell} \; v' \lesssim 10^{-10} \text{ GeV}. \tag{2}$$

‡Electronic address: zgsi@sdu.edu.cn

§Electronic address: wangkai@hep.wisc.edu

This implies a stringent bound on v'. For instance, if we take $Y_{\ell\ell}$ to be as small as the electron's Yukawa coupling, we have $v' \sim 10^{-2}$ MeV. As for any $\Delta L = 2$ interactions, neutrinoless double beta decay experiments ($0\nu\beta\beta$) [11] provide a direct test. H^{++} also contributes to $0\nu\beta\beta$ via $W^-W^- \to H^{--} \to \ell^-\ell^-$. The $W^-W^-H^{++}$ coupling is proportional to v' in the model under discussion, and with the $0\nu\beta\beta$ bound [12, 13, 14], we have

$$\frac{v' Y_{\ell\ell}}{m^2_{H^{++}}} \leq 5 \times 10^{-8}\ \text{GeV}^{-1}. \tag{3}$$

Given the neutrino mass requirement in Eq. (2), we obtain a bound $m_{H^{++}} > 0.1$ GeV, which is too weak to be relevant here.

In fact, there is another direct bound on v' due to the electroweak ρ-parameter. In order to prevent large tree-level contributions to the ρ-parameter, one needs [10, 15] $v' \lesssim 1$ GeV. Although models exist in the literature [2, 15, 16], where one has complex as well as real triplets, whose combined contributions to the ρ-parameter cancel, thus allowing large triplet vevs at the tree level, they presuppose the existence of additional symmetries whose validity is not clear once higher order effects involving gauge couplings are included.

It is also to be noted that, if v' is allowed to be close to the upper limit from the ρ-parameter, then the couplings $Y_{\ell\ell}$ are forced to be $\simeq 10^{-10}$. Since there are six of these couplings (assuming the matrix to be real symmetric), they all need to be adjusted within such a small range in order to reproduce the neutrino mass matrix that fits the observed mixing pattern. This makes the scenario rather more fine-tuned than one in which one has a much smaller v' a single quantity), along with the six parameters $Y_{\ell\ell}$ which are allowed to be closer to unity. In this phenomenological study, we will assume a small v' and be guided for the parameters by the neutrino mass generation, to saturate the relation of Eq. (2).

Secondly, we wish to identify the leading production channels for the doubly charged Higgs at the LHC. Rather encouraging predictions about single production of the doubly charged Higgs boson in W-boson fusion can be found in some earlier studies via the process $W^+W^+ \to H^{++}$ [15, 16, 17, 18, 19, 20]. However, specific features of models are often utilized in such studies, and it is difficult to maintain such optimism in a general case if the triplet vev is restricted to a smaller value. Numerically, the signal rate is proportional to $(v'/v)^2$ and is already too small to be observable at the LHC if $v' \lesssim 1$ GeV. Since we are considering even smaller values of v', we therefore concentrate instead on pair production which is largely governed by electromagnetic interactions. In principle, the production of

one doubly-charged Higgs in conjunction with a singly charged one, followed by the decay $H^{++} \longrightarrow H^+W^+$, driven by the $SU(2)_L$ gauge coupling, can generate additional signals [21]. However, this presupposes considerable mass separation between the H^{++} and the H^+, which may not be quite expected in many scenarios such as those based on Little Higgs theories. Therefore, we concentrate on the pair production process as the constantly available fall-back, and remember that the doubly charged scalars produced most copiously in the Drell-Yan (DY) channel. In our analysis, we also include the production via the two-photon fusion channel. This is motivated by the stronger electromagnetic coupling of a doubly charged particle. Comparing with a singly charged scalar, the two-photon channel will have an enhancement factor of 16. Numerically, it provides about 10 per cent correction to the DY process, and it is comparable to the QCD corrections [22].

Thirdly, as for the identification of the $H^{\pm\pm}$ signal, one must consider both $H^{++} \to \ell^+\ell^+$ and $H^{++} \to W^+W^+$, keeping in mind the interplay of the two independent parameters $Y_{\ell\ell}$ and v' that govern the two decay channels. In spite of the simple and distinctive nature of the first signal, one cannot rule out their faking by a number of sources. We have studied in detail the event selection criteria which establish the *bona fide* of such signals in a convincing way. Side by side, we are also suggesting ways of isolating the signals coming from $H^{++} \to W^+W^+$, which are in general more background-prone, and can dominate the decays of the doubly charged scalar in certain regions of the parameter space. Most studies on the signals of doubly charged scalars have not adequately addressed the challenges posed by backgrounds in this search channel. Furthermore, given the small values of $Y_{\ell\ell}v'$, it is useful to investigate whether the doubly charged Higgs can indeed be long-lived on the scale of collider detectors in any region of the parameter space of this scenario, a situation experimentalists have already looked for at the Tevatron [6]. And finally, we wish to point out, albeit in a qualitative way, that relative strengths of the different flavor diagonal as well as off-diagonal decays $H^{++} \to \ell_i^+\ell_j^+$ of the doubly charged state should give us information about the matrix $Y_{\ell\ell}$ and, in turn, generate insight into the structure of the neutrino mass matrix [8], which is responsible for the tri-bimaximal mixing pattern suggested by observations.

We present the calculation related to both the Drell-Yan and two-photon production channels at the LHC in Sec. II. Section III contains a discussion on the decay of the doubly charged states into the $\ell^\pm\ell^\pm$ and $W^\pm W^\pm$ final states across the parameter space allowed by the neutrino mass constraint. The signal observability at the LHC for both channels are

discussed in detail in Sec. IV. We summarize and conclude in Sec. V.

II. PRODUCTION AT HADRON COLLIDERS

A. Drell-Yan production

As has been already discussed in the literature, the dominant chanel through which doubly charged scalar pairs can be produced at hadron colliders is the Drell-Yan process

$$q(p_1) \,+\, \bar{q}(p_2) \,\rightarrow\, H^{++}(k_1) \,+\, H^{--}(k_2), \tag{4}$$

In terms of $y = \hat{\mathbf{p}}_1 \cdot \hat{\mathbf{k}}_1$ in the parton c.m. frame, the parton level differential cross section for this process is

$$\begin{aligned}\frac{d\sigma}{dy} \;=\; & \frac{16\pi\alpha^2\beta^3(1-y^2)}{N_c s}\Big\{e_q^2 \,+\, \frac{s}{(s-M_Z^2)^2+\Gamma_Z^2 M_Z^2}\,\frac{\cos 2\theta_W}{\sin 2\theta_W} \\ & \times\Big[2e_q g_V^q (s-M_Z^2) \,+\, (g_V^{q2}+g_A^{q2}) s\,\frac{\cos 2\theta_W}{\sin 2\theta_W}\Big]\Big\},\end{aligned} \tag{5}$$

where $\beta = \sqrt{1-4m_H^2/s}$ is the speed of H^{++} in the c.m. frame.

The QCD corrections to this process have been also computed, yielding a next-to leading order (NLO) K-factor of the order of 1.25 at the LHC energy for the entire mass range between 200 GeV and 1 TeV [22].

B. Two-photon fusion

Due to the stronger electromagnetic coupling of the doubly charged scalar, one may anticipate a sizable two-photon contribution to the pair production. Comparing with a singly charged scalar, the two-photon channel will have an enhancement factor of 16. We consider the dominant contribution from the collinear photons and adopt the effective photon approximation. The event rates from effective photon contributions can be just added to the Drell-Yan contributions to the $H^{++}H^{--}X$ final state .

For the process

$$\gamma(p_1) \,+\, \gamma(p_2) \,\rightarrow\, H^{++}(k_1) \,+\, H^{--}(k_2), \tag{6}$$

the matrix element squared is

$$|\mathcal{M}|^2 = \frac{128\,e^4\,\left(1-2\,\beta^2+\beta^4\,\left(2-2\,y^2+y^4\right)\right)}{\left(-1+\beta^2\,y^2\right)^2}. \tag{7}$$

The corresponding differential cross section can be obtained as

$$\frac{d\sigma}{dy} = \frac{16\pi\,\alpha^2\,\beta\,\left(1-2\,\beta^2+\beta^4\,\left(2-2\,y^2+y^4\right)\right)}{s\left(-1+\beta^2\,y^2\right)^2}. \tag{8}$$

It is interesting to see the different β-dependence of the cross sections for the DY and two-photon processes. The DY process undergoes a pure P-wave channel, while the two-photon process contains all $S,\ P,\ D$ waves leading to a general dependence of β^{2l+1} near the threshold.

Furthermore, the two-photon contributions may arise from both elastic and inelastic processes, including the semi-elastic case where it is elastic on one side and inelastic on the other. The total cross-section can thus be written as [23]

$$\sigma_{\gamma\gamma} = \sigma_{\rm elastic} + \sigma_{\rm inelastic} + \sigma_{\rm semi-elastic} \tag{9}$$

where the elastic channel is the photon radiation off a proton, and the inelastic channel is that off a quark parton. The semi-elastic is the product of both. They are given by

$$\sigma_{\rm elastic} = \int_\tau^1 dz_1 \int_{\tau/z_1}^1 dz_2 f_{\gamma/p}(z_1) f_{\gamma/p'}(z_2)\sigma(\gamma\gamma\to H^{++}H^{--}), \qquad \tau = \frac{4m^2}{S}, \tag{10}$$

$$\sigma_{\rm inelastic} = \int_\tau^1 dx_1 \int_{\tau/x_1}^1 dx_2 \int_{\tau/x_1/x_2}^1 dz_1 \int_{\tau/x_1/x_2/z_1}^1 \tag{11}$$

$$dz_2 f_q(x_1) f_q'(x_2) f_{\gamma/q}(z_1) f_{\gamma/q'}(z_2)\sigma(\gamma\gamma\to H^{++}H^{--}) \tag{12}$$

$$\sigma_{\rm semi-elastic} = \int_\tau^1 dx_1 \int_{\tau/x_1}^1 dz_1 \int_{\tau/x_1/z_1}^1 dz_2 f_q(x_1) f_{\gamma/q}(z_1) f_{\gamma/p'}(z_2)\sigma(\gamma\gamma\to H^{++}H^{--}). \tag{13}$$

We employ the frame structure functions following reference [23]:

$$f_{\gamma/q}(z) = \frac{\alpha_{\rm em}}{2\pi}\frac{1+(1-z)^2}{z}\ln(Q_1^2/Q_2^2) \tag{14}$$

$$f_{\gamma/p}(z) = \frac{\alpha_{\rm em}}{2\pi z}(1+(1-z)^2)\left[\ln A - \frac{11}{6} + \frac{3}{A} - \frac{3}{2A^2} + \frac{1}{3A^3}\right] \tag{15}$$

$$A = 1 + \frac{0.71\ {\rm GeV}^2}{Q^2_{\rm min}} \tag{16}$$

$$Q^2_{\rm min} = -2m_p^2 + \frac{1}{2s}\left[(s+m_p^2)(s-zs+m_p^2) - (s-m_p^2)\sqrt{(s-zs-m_p^2)^2-4m_p^2 zs}\ \right]. \tag{17}$$

The treatment in this section has ignored the channels from other gauge boson fusions such as $W^*,\ Z^*,\ \gamma^*$ (virtual in general). Our estimates reveal that the production through W-fusion channel is rather suppressed and more so for Z-fusion. The cost of using the effective photon approximation rather than calculating the full $2\to 4$ subprocess is the loss

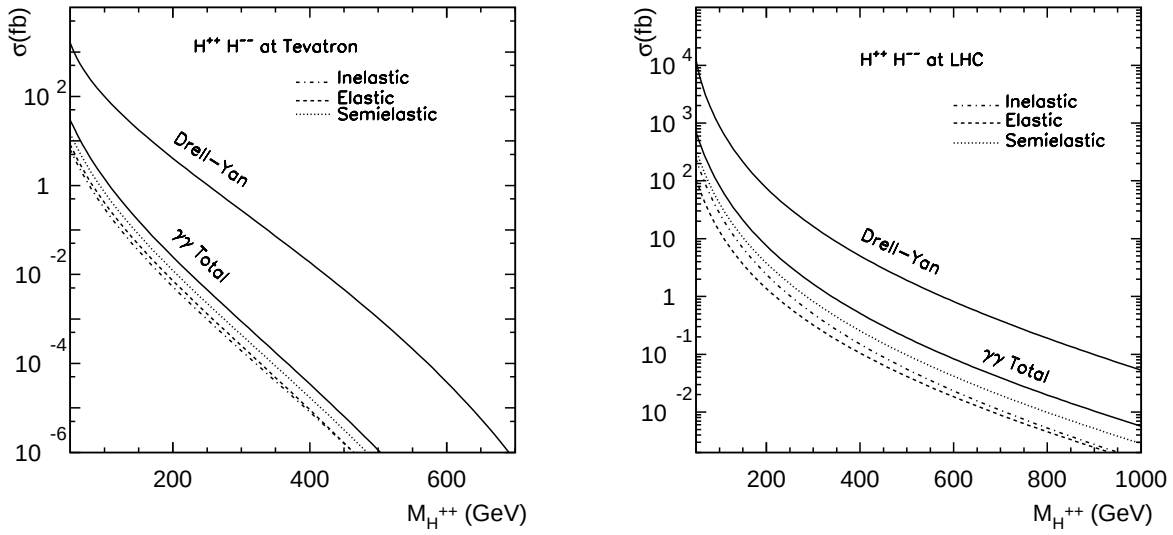

FIG. 1: Production rates for the doubly charged Higgs pair at the Tevatron (left) and the LHC (right), in the leading order Drell-Yan and two-photon (semi-elastic, elastic, and inelastic) channels.

of the potential tagging jets in the forward-backward regions. Fortunately, due to the rather clean charged leptonic final states, we do not require such jet tagging to identify the signal.

C. Numerical results

In Fig. 1 the total cross-sections are plotted against the mass of the doubly charged scalar, showing the Drell-Yan as well as different types of the two-photon processes. The highest lower bound on a doubly charged Higgs mass from the Tevatron search with an integrated luminosity of 240 pb^{-1} is about 136 GeV (though in the specific context of a left-right symmetric model). It can be seen from Fig. 1 that with 10 fb^{-1} at the Tevatron, the mass reach may be extended approximately to 250 GeV. At the LHC, the production rate is increased by a factor of 20 over that at the Tevatron, reaching the order of femtobarns for a Higgs mass upto as much as 600 GeV, and of 0.1 fb for a mass of 1 TeV. We have also shown the three classes of contributions from the two-photon channel separately. It is interesting to note that the rate of the elastic process is larger than that of the inelastic at the Tevatron energies, while the pattern is reversed at the LHC energies. This is because the probability of a proton remaining unbroken after the emission of a photon in an elastic

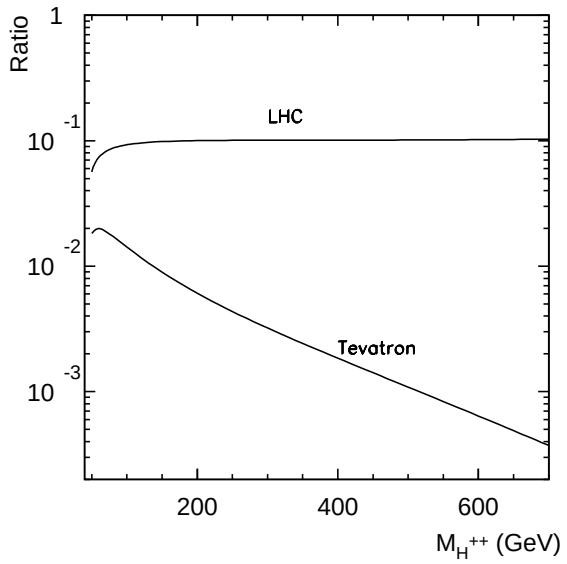

FIG. 2: The ratio between $\sigma_{\gamma\gamma}$ and leading order $\sigma_{\rm DY}$ at the LHC and the Tevatron.

process is smaller at the LHC. The semi-elastic contribution is numerically the highest in both cases, because of a factor of 2 for the initial state interchanges. The ratio of the two-photon contribution relative to the Drell-Yan channel is shown in Fig. 2. In general, the two-photon contributions at LHC remain about 10% of that of the Drell-Yan process, while the fraction is much smaller for the Tevatron, the reason being that is the photon needs to come with a larger momentum fraction of the parent parton in the latter case, for which the distribution function is relatively suppressed. It should be noted that, while the Drell-Yan cross-section has a next-to-leading order (NLO) QCD K-factor of about 1.25 [22], only the leading order cross-section has been presented in these figures. This is for comparison of the correction to this cross-section due to the two-photon process and the strong correction mentioned above. Higher order corrections to the two photon electromagnetic process are rather small. CTEQ6L parton distribution functions have been used in the calculation, and the factorization scale is set at half the subprocess center-of-mass energy $\sqrt{s}/2$.

We now examine some kinematic features of the two processes considered above. As shown in Fig. 3, while the transverse momentum (p_T) of the scalars tends to peak at values that are significant fractions of its mass, Drell-Yan production leads to scalars with harder p_T distributions than those from the two-photon fusion. This is due to the forward-backward

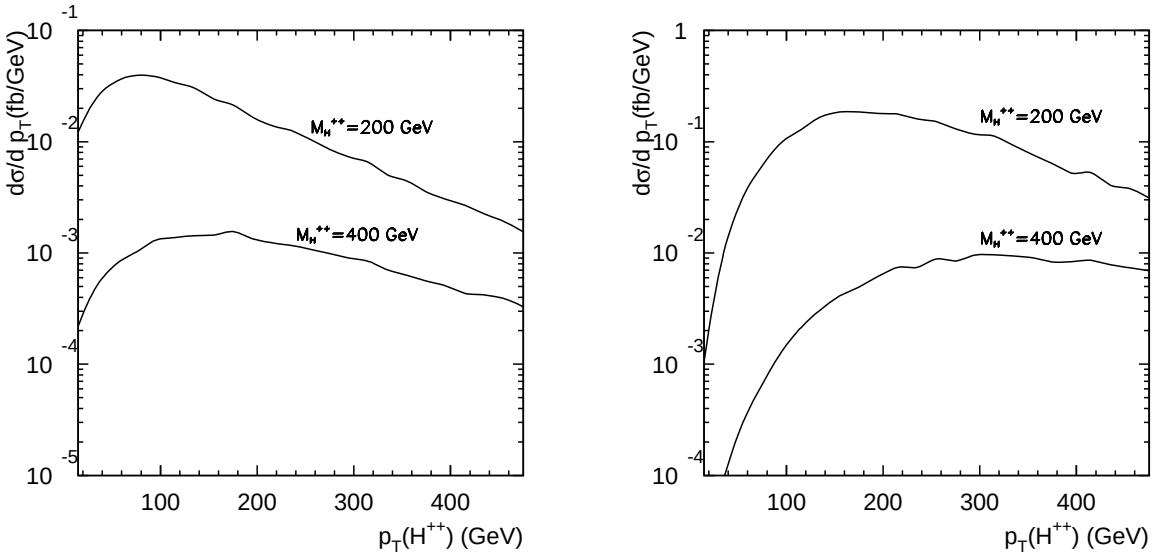

FIG. 3: Transverse momentum distributions of the doubly charged Higgs produced in the two-photon (left) and Drell-Yan (right) channels at the LHC.

nature of the $t,\ u$-channels in the two-photon process at high energies. The rapidity (η) distributions in Fig. 4 reflect central peaking for both channels, and the distributions are broader for the two-photon process. On the whole, in spite of some qualitative differences between these two channels, it is not possible effectively to separate the two production mechanisms through the kinematical considerations. In our subsequent analysis, we will add them up incoherently.

III. DECAYS OF THE DOUBLY CHARGED HIGGS

The doubly charged Higgs may in principle decay into all of the following two-body final states:

$$H^{++} \to \ell_i^+ \ell_j^+, \quad H^{++} \to W^+ W^+.$$
$$H^{++} \to H^+ W^+, \quad H^{++} \to H^+ H^+.$$

The third and fourth channels depend on the mass splitting among the members of the triplet, and also the scalar potential. The consequence of the third channel being kinematically allowed (which makes it the dominant decay, since it is driven by the $\mathrm{SU}(2)_L$ gauge

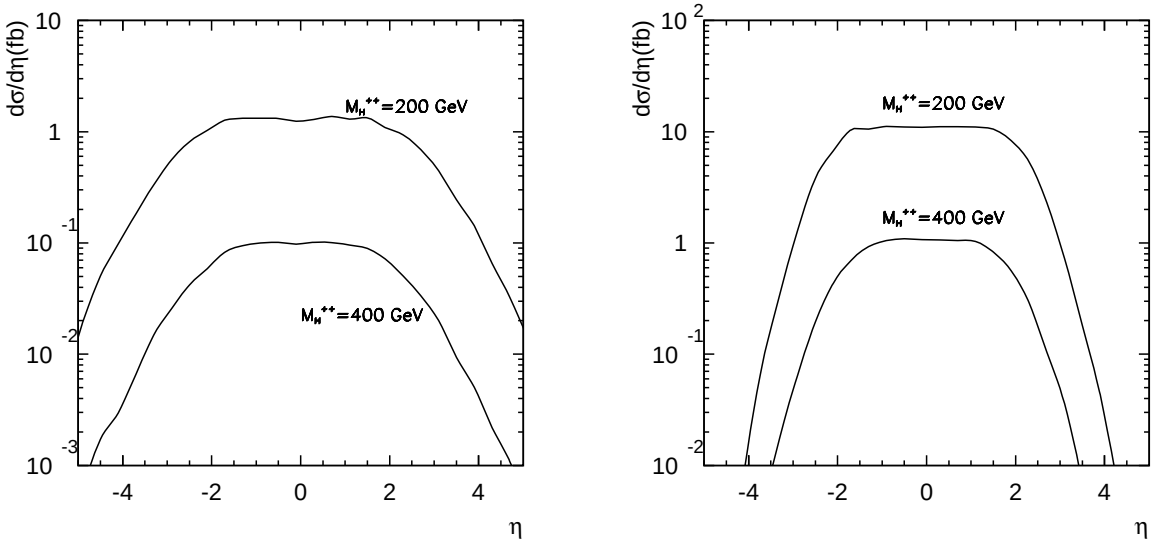

FIG. 4: Rapidity distributions of the doubly charged Higgs produced in the two-photon (left) and Drell-Yan (right) channels at the LHC.

coupling) has been discussed, for example, in reference [24], in the context of a linear collider. Here we take a conservative approach and assume that the mass splitting within the triplet is very small as is the case, for example, in Little Higgs models. Thus only the first two decays listed above occur in our scenario,[1] the corresponding widths being given by [9]

$$\begin{aligned}
\Gamma(H^{++} \to \ell_i^+ \ell_j^+) &= \frac{1}{4\pi(1+\delta_{ij})} |Y_{\ell\ell}^{ij}|^2 M_{H^{++}} \ , \\
\Gamma(H^{++} \to W_T^+ W_T^+) &= \frac{1}{4\pi} \frac{g^4 v'^2}{M_{H^{++}}} \frac{\lambda^{\frac{1}{2}}(1, r_W^2, r_W^2)}{\sqrt{4r_W^2 + \lambda(1, r_W^2, r_W^2)}} \approx \frac{g^4 v'^2}{4\pi M_{H^{++}}}, \\
\Gamma(H^{++} \to W_L^+ W_L^+) &= \frac{1}{4\pi} \frac{g^4 v'^2}{2M_{H^{++}}} \frac{\lambda^{\frac{1}{2}}(1, r_W^2, r_W^2)}{\sqrt{4r_W^2 + \lambda(1, r_W^2, r_W^2)}} \frac{(1-4r_W^2)^2}{4r_W^4} \approx \frac{v'^2 M_{H^{++}}^3}{2\pi v^4}.
\end{aligned} \quad (18)$$

in terms of the kinematic function $\lambda(x,y,z) = x^2 + y^2 + z^2 - 2xy - 2xz - 2yz$ and the scaled mass variable $r_W = M_W/M_{H^{++}}$. The approximate forms are valid for $M_{H^{++}} \gg M_W$. The subscripts T and L denote the transverse and longitudinal polarizations of the W boson.

[1] The omission of the $H^\pm W^\pm$ mode will affect neither our analyses nor the results for the individual channels $\ell^\pm\ell^\pm$ and $W^\pm W^\pm$, since the branching ratios in these channels have been used by us as free parameters. However, the inclusion of this mode can in principle alter the overall discovery limit, depending upon the mass parameters.

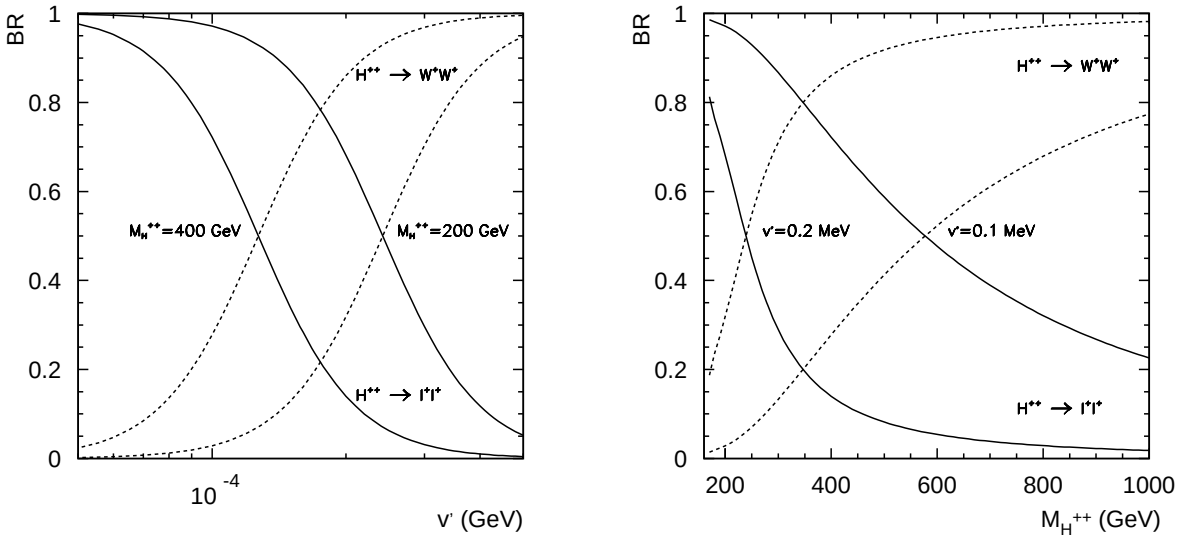

FIG. 5: Branching fractions for $H^{++} \to \ell^+\ell^+$ ($e^+e^+ + \mu^+\mu^+ + \tau^+\tau^+$) and $H^{++} \to W^+W^+$ as functions of (left) the triplet vev, for two values of the doubly charged Higgs mass, and (right) the Higgs mass for two choices of v'.

The longitudinal W final state becomes dominant at higher $M_{H^{++}}$.

The relative strengths of the two types of decays ($\ell^+\ell^+, W^+W^+$) depend on the couplings $Y_{\ell\ell}$ as well the triplet vev v', which has to be less than 1 GeV in order to prevent large tree-level contributions to the ρ-parameter unless additional model assumptions are made. While treating $Y_{\ell\ell}$ and v' as completely free parameters can lead to practically any relative strength between the two sets of final states, we have been guided by the additional constraint of neutrino mass generation, to saturate the bound of Eq. (2). Of course, $Y_{\ell\ell}v'$ can be even smaller if there are right-handed neutrinos in addition, for instance, a Type II seesaw mechanism is operative. We shall further comment on this possibility at the end of this section. In Fig. 5 we show the branching fractions for the $\ell^+\ell^+$ ($e^+e^+ + \mu^+\mu^+ + \tau^+\tau^+$) and W^+W^+ decay modes as functions of the triplet vev (left) and the Higgs mass (right), keeping the overall constraint from neutrino mass mentioned above. With a higher mass of H^{++}, the W^+W^+ mode overtakes $\ell^+\ell^+$ sooner due to the fast growing W_LW_L mode, even for a relatively smaller value of v'. While the explanation is obvious from the expressions of the decay widths, this underlines the importance of exploring the latter mode at LHC, in addition to the easily identifiable like-sign lepton pair signal.

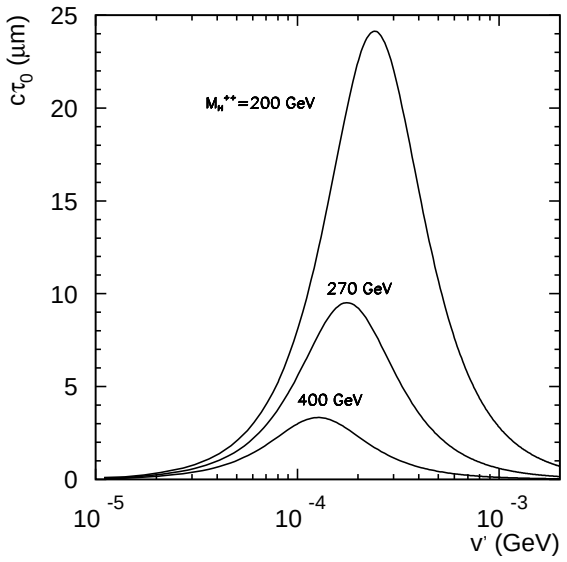

FIG. 6: The proper decay length $c\tau_0$ in units of μm for the doubly charged Higgs as a function of the triplet vev, within the neutrino mass constraint.

Since $Y_{\ell\ell}$ and v' are both quite small, it is natural to ask whether the decay width of H^{++} can be so small that it becomes quasi-stable in the collider experiments. As has been mentioned earlier, a long-lived doubly charged Higgs has been looked for at the Tevatron, in terms of highly ionizing tracks and muon-like penetration beyond the electromagnetic and hadron calorimeters [6]. In Fig. 6, we plot the the proper decay length $c\tau_0$ with τ_0 being the proper lifetime of H^{++}, keeping within the constraint on $Y_{\ell\ell}v'$ from neutrino mass to saturate Eq. (2). It can be seen that, for a light scalar $M_{H^{++}} < 270$ GeV with certain values of v', the proper decay length may exceed 10 microns. Such a decay length can be enhanced to a visible displaced secondary vertex by the appropriate boost $\beta\gamma = p/M$. The length goes further down for a more massive scalar. Thus it can be concluded that a doubly charged Higgs cannot be long-lived, or quasi-stable, on the scale of a collider detector if its $\Delta L = 2$ coupling has to be the mechanism operative for the generation of neutrino masses. The observation of a long-lived H^{++} should therefore tell us that something over and above the $\Delta L = 2$ interaction is active for generating neutrino masses.

It should also be remembered that $Y_{\ell\ell}^{ij}$ can have six independent elements (assuming a real symmetric Majorana neutrino mass matrix) in general. Values of these elements are highly model-dependent and they can lead to a wide number of possibilities in flavor diagonal as

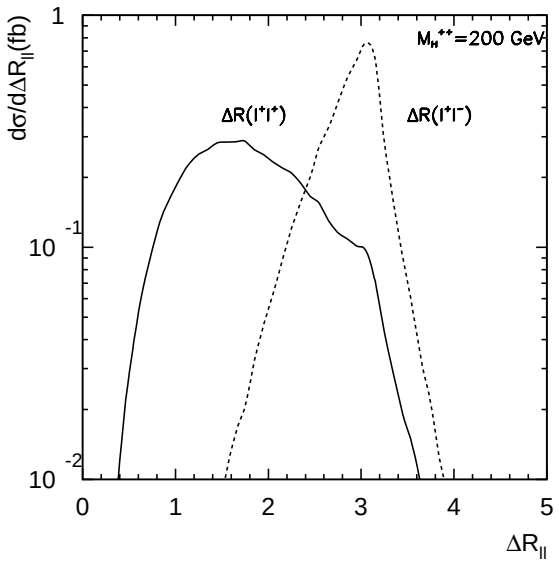

FIG. 7: $\Delta R_{\ell\ell}$ distributions for same-sign (solid) opposite-sign (dotted) dileptons in the four-lepton final state. For opposite-sign dileptons, the isolation between the two harder leptons of each sign has been selected.

well as off-diagonal decays of the H^{++}. While there is very little guideline as to the choice of these values, it should be emphasized that actual observation of the decays into different flavor combinations can actually give us information about the structure of the neutrino mass matrix. In order to convey the general features of the collider analysis, we assume a diagonal structure of ${Y_{\ell\ell}}^{ij}$, with the same value for all three flavors, as shown in Fig. 5. We include only the electronic and muonic branching ratios added together while predicting the signal events at the hadron colliders. This analysis can always be translated into one with a variety of structures for the $Y_{\ell\ell}^{ij}$, without any serious difference in the results presented here.

IV. PREDICTION OF EVENTS AT THE LHC

A. Like-sign dilepton pairs

We first consider the most spectacular final state, namely,

$$pp \to H^{++}H^{--} \to \ell^+\ell^+\ \ell^-\ell^-\ (\ell = e,\ \mu), \tag{19}$$

driven by the decay of the H^{++} into lepton pairs. As mentioned earlier, we have assumed the same branching ratio for flavor diagonal decays into the three lepton channels, and included the electron and muon pairs as our characteristic signals. The branching ratio into lepton pairs has been taken as a free parameter, since, given the neutrino mass constraint, the decay rate into W^+W^+ is automatically determined by it.

We consider both electrons and muons. To simulate the detector effects on the energy-momentum measurements, we smear the electromagnetic energy and the muon momentum tracking by a Gaussian distribution whose width is [25]

$$\frac{\Delta E}{E} = \frac{a_{cal}}{\sqrt{E/\mathrm{GeV}}} \oplus b_{cal}, \quad a_{cal} = 10\%,\ b_{cal} = 0.4\%, \tag{20}$$

$$\frac{\Delta p_T}{p_T} = \frac{a_{track}\ p_T}{\mathrm{TeV}} \oplus \frac{b_{track}}{\sqrt{\sin\theta}}, \quad a_{track} = 36\%,\ b_{track} = 1.3\%. \tag{21}$$

The signal consists of two like sign dilepton pairs with the same invariant mass. As can be seen from Fig. 7, the ΔR distribution (where $\Delta R^2 = \Delta\eta^2 + \Delta\phi^2$) of the like-sign pairs peaks at a smaller value than that of opposite sign dileptons, thereby indicating a spatial separation of the pairs, at least when the doubly charged scalars are sufficiently boosted. We have checked that this separation remains noticeable well beyond $M_{H^{++}} \simeq 400 - 500$ GeV. In addition, we have employed the following acceptance criteria for the events:

- A veto on any opposite sign dilepton pair invariant mass being close to the Z-boson mass: $|m(\ell^+\ell^-) - M_Z| > 15$ GeV.
- $p_T(\ell) > 15$ GeV, and the hardest leptons has $p_T(\ell_{hard}) > 30$ GeV.
- $|\eta(\ell)| < 2.8$.

The above signal has *prima facie* no standard model background. However, fake backgrounds may arise from W bosons in conjunction with misidentified jets and/or leptons from heavy flavor decays. In order to suppress such backgrounds, we recommend the following steps:

- Reconstruct the invariant mass of each like-sign dilepton pair, and insist on their being equal within about 5 per cent. While the smearing procedure is seen to keep the invariant masses of the signal pairs equal well within this limit, backgrounds are largely eliminated by it.

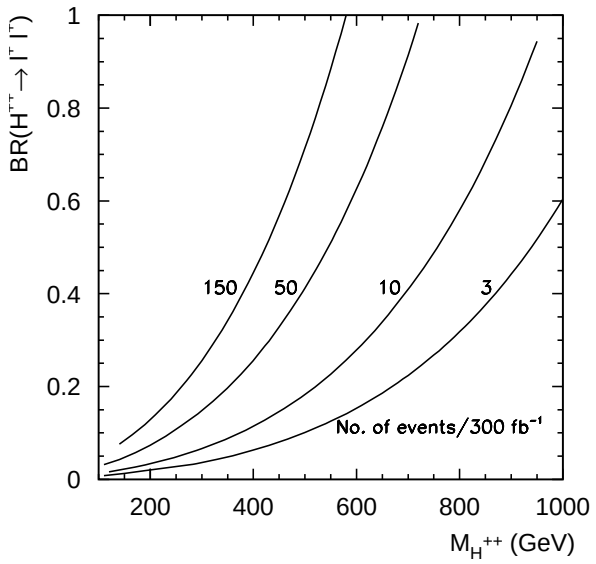

FIG. 8: Equal event contours in the BR($H^{++} \to \ell^+\ell^+$) – M_H^{++} plane, including the cuts discussed in the text, for an integrated luminosity of 300 fb^{-1}.

- Demand a minimum ΔR-isolation of 0.5 between each lepton and any nearby jet.
- Demand little missing transverse energy: $\not{E}_T < 25$ GeV.

In Fig. 8 we present event contours in the space spanned by the H^{++} mass and the branching fraction $BR(H^{++} \to \ell^+\ell^+)$ for an integrated luminosity of 300 fb^{-1}. The Drell-Yan contribution has been multiplied here by the NLO K-factor 1.25, and the two-photon contribution has also been included. In the absence of backgrounds after all of the cuts discussed above, the contour corresponding to three events can be taken as the 99% C.L. discovery limit for an integrated luminosity of 300 fb^{-1}. The event rates suggest a high degree of detectability of the signal, even for rather small branching ratios. Given the acceptance criteria listed above, it can be concluded from the contours that a doubly charged Higgs up to the mass range of 1 TeV can be detected at the LHC if the $\ell^+\ell^+$ decay mode has a branching ratio on the order of 60 per cent. On the lower side, even a branching ratio of 10 (5) per cent allows a 99% C.L. search limit of 500 (350) GeV. A recent similar study has appeared [26] for the DY process and the leptonic decay mode of H^{++} only. Their numerical results, wherever overlapping, are in agreement with ours.

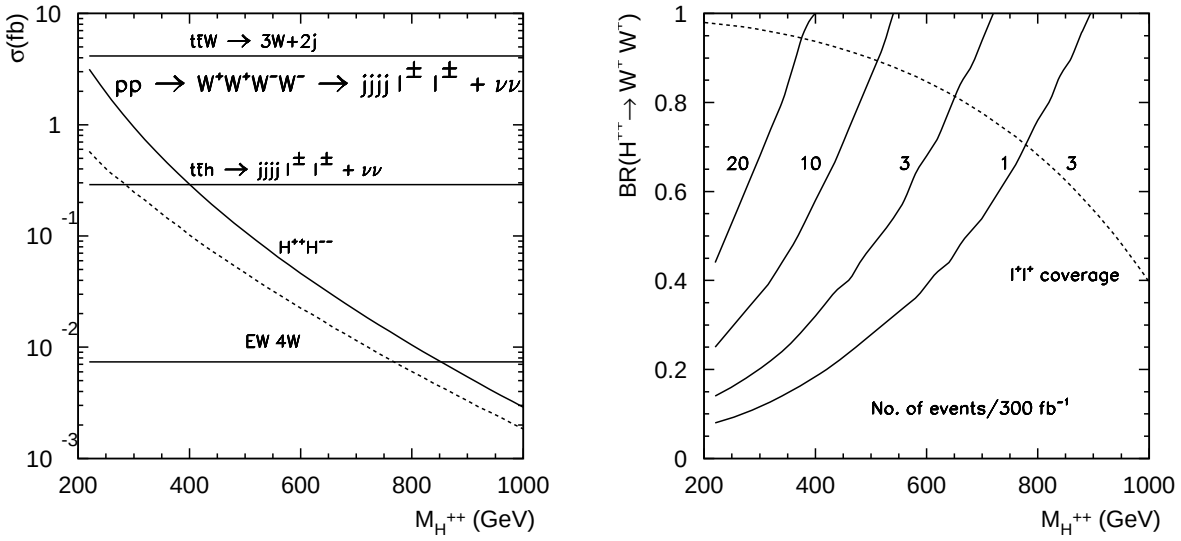

FIG. 9: (a) Left: Total cross sections for $jjjj\ell^\pm\ell^\pm + \not{E}_T$ events. The solid (dotted) line corresponds to event rates coming from each doubly charged scalar decaying into two like-sign W's without (with) basic cuts as described in the text. Event rates from various types of background are also shown, without the basic cuts. (b) Right: Equal event contours in the BR($H^{++} \to W^+W^+$)$-M_H^{++}$ plane, including the cuts discussed in the text, for an integrated luminosity of 300 fb^{-1}. The dashed curve is a reproduction of the 3-event contour in Fig. 8.

B. Like-sign W-pairs

Next, let us consider the W^+W^+ channel. As can be seen from Fig. 5, this channel may become dominant even for rather small values of the triplet vev, especially if the H^{++} mass is on the higher side. It is therefore desirable to devise search strategies for this channel, leading to a final state consisting of $W^+W^+W^-W^-$. In order to confirm the nature of a doubly charged state, and to reveal its resonant production, we propose to reconstruct the events by looking for two like-sign W's through a pair of like-sign dileptons and the remaining two in their hadronic decays which allow complete reconstruction of $M_{H^{++}}$. The branching fraction for this decay chain is taken to be

$$\text{BR}(W^+W^+W^-W^- \to \ell_i^\pm\nu\ \ell_j^\pm\nu\ 4j) \approx 2\ (\frac{2}{9})^2\ (\frac{6}{9})^2 \approx 4.4\%. \tag{22}$$

The predicted cross sections including the above branching fraction are shown in Fig. 9(a), assuming BR($H^{++} \to W^+W^+$) to be 100%. The rather small branching fraction in Eq. (22)

is a price we pay for cleaner signals, and consequently the event rate tends to be low for a high H^{++} mass. For instance, it may only have a handful events for $M_{H^{++}} \sim 1$ TeV with an integrated luminosity of 300 fb^{-1}, even before any acceptance cuts.

We again start with some "basic cuts", where the leptons are subject to the same acceptance criteria as before. In addition, we demand

- $\not{E}_T > 40$ GeV
- $p_T(j) \geq 30$ GeV, $|\eta(j)| \leq 3.0$.

The jet energies are also smeared using the same Gaussian formula [25] as in Eq. (20), but with

$$a = 80\%, \quad b = 15\%. \tag{23}$$

As seen from the solid and dotted curves in Fig. 9(a), these criteria do not affect the signal in a significant way, especially for heavier masses. In Fig. 9(b) we translate the signal cross section to equal event contours in the BR($H^{++} \to W^+W^+$) $- M_H^{++}$ plane, including the cuts discussed above and both $\ell^+\ell^+$ and $\ell^-\ell^-$, for an integrated luminosity of 300 fb^{-1}. For comparison, we reproduce the 3-event contour in Fig. 8 by the darshed curve, assuming BR($H^{++} \to \ell^+\ell^+$) $= 1 -$ BR($H^{++} \to W^+W^+$). This illustrates the complementarity between these two channels for different values of the BR's.

As for the SM backgrounds, the purely electroweak production of $4W$ final states is rather modest [27], as indicated in Fig. 9(a) with the branching fraction of Eq. (22) included. A next background leading to $4W$ final states from $t\bar{t}$ $t\bar{t}$ production [28] is larger but the kinematics will look very different from the signal processes due to the four extra hard b jets. It is easy to demonstrate that these backgrounds can be effectively suppressed well below the signal by judicial kinematical cuts.

The largest background arises from $t\bar{t}W$ production. In addition, if the $WW^{(*)}$ mode from the SM Higgs boson (h) has a substantial branching ratio, then the $t\bar{t}h$ production [28, 29] may constitute a severe background. As shown in [29], this production cross-section for $t\bar{t}h$ can be of the order of 150 fb for a Higgs mass of 200 GeV when it has unsuppressed decays into two W's, and this can contribute enough 4-jet plus like-sign dilepton events to swamp our signals. We have found that the event selection strategies which can suppress the leading $t\bar{t}W$ background are also effective in reducing the fake events coming from $t\bar{t}h$.

Therefore, we outline below a step-by-step procedure for reducing the leading background, as summarised in Table I. The relatively smaller backgrounds of $4t$ and $4W$ are also taken care of by the same procedure. For illustration, we first choose a doubly-charged Higgs mass of 300 GeV. In the results presented, the branching ratio for $H^{++} \to W^+W^+$ has been taken as unity.

First of all, we wish to select events with four jets and thus we veto events with additional central jets in the region,

$$|\eta^{veto}(j)| < 3,\ p_T^{veto}(j) > 30 \text{ GeV}.$$

Then we experiment with progressively stronger cuts on the (leading) lepton and jet p_T. Furthermore, the four jets will pair up to reconstruct two M_W peaks, and we thus demand $|M_{j_1 j_2} - M_W| < 15$ GeV for the pair closest to the M_W peak and the other pair at the same time. As seen from the table, this reduces both the $t\bar{t}W$ and $t\bar{t}h$ backgrounds rather drastically, but not to the extent necessary for discerning the signal. Therefore, one should note that the pair production of the heavy Higgs bosons has a high energy threshold. We accordingly define a cluster transverse mass for the whole system

$$M_{cluster} = \sqrt{m_{4j}^2 + (\sum \vec{p_T}^{\,j})^2} + \sqrt{m_{\ell\ell}^2 + (\sum \vec{p_T}^{\,\ell})^2} + \not{E}_T \tag{24}$$

which should start from a threshold around $2M_{H^{++}}$. We impose a cut of 600 GeV on this variable. For the $H^{\pm\pm}$ kinematics on the leptonic side, we can only define a transverse mass due to the missing neutrinos

$$M_T = \sqrt{(\sqrt{m_{\ell\ell}^2 + (\sum \vec{p_T}^{\,\ell})^2} + \not{E}_T)^2 - (\sum \vec{p_T}^{\,\ell} + \vec{\not{E}}_T)^2}. \tag{25}$$

and a cut of 300 GeV on this quantity proves to be effective in further reducing the background. On the hadronic side, the 4-jet invariant mass should peak at the location of $M_{H^{++}}$. Taking into account the detector resolution, we look for the events in the window $M_{H^{++}} \pm 50$ (30) GeV, which reduces the background by another order of magnitude. Two sets of numerical values for the cuts have been presented in Table I, to establish the fact that the successive criteria applied here can reduce the backgrounds by more than two orders of magnitude, while the survival efficiency for the signal remains as high as 35%. This example illustrates how the rather distinctive kinematical features of the signal allow us to effectively suppress the SM backgrounds, after which the signal observation is mainly a statistical issue.

(fb)	Basic Cuts	p_T^ℓ cut	p_T^j cut	M_W reconst.	$M_{\rm Cluster}$	M_T	M_{jjjj}
cuts	$\not{E}_T > 40$ GeV	> 70 GeV	> 120 GeV	$M_W \pm 15$ GeV	> 600 GeV	> 300 GeV	300 ± 50 GeV
signal	0.20	0.17	0.15	0.13	0.13	0.12	0.12
$t\bar{t}W$	4.15	2.52	1.60	0.82	0.74	0.48	0.12
cuts	$\not{E}_T > 70$ GeV	> 120 GeV	> 120GeV	$M_W \pm 15$ GeV	> 600 GeV	< 300 GeV	300 ± 30GeV
signal	0.17	9.71×10^{-2}	9.08×10^{-2}	8.27×10^{-2}	8.24×10^{-2}	7.80×10^{-2}	6.18×10^{-2}
$t\bar{t}W$	2.82	0.79	0.62	0.32	0.30	0.15	2.90×10^{-2}

TABLE I: The signal and the leading background rates for $pp \to W^+W^+W^-W^- \to jjjj + \ell^+\ell^+ + \not{E}_T$. The rates after imposing each selection criterion, as described in the text, are shown. $m_{H^{++}} = 300$ GeV. $\mu_R = \mu_F = (2m_t + M_W)/2$ for $t\bar{t}W$ calculation.

If the doubly charged Higgs is heavier, the W's arising from its decay will be boosted, so that the two jets from each of the hadronically decaying ones are rather highly collimated. The typical opening angle of each pair from W-decay resulting into a single fat jet of this kind is $2M_W/M_{H^{++}} \approx 0.27$ for $M_{H^{++}} = 600$ GeV, and the peak in ΔR bwteen jets coming from the hadronically decaying W's occurs around 0.4. This means that a substantial fraction of the four parton-level jets for such a high Higgs mass will actually be merged into two-jet events, together with the like-sign dileptons. Such final states are apparently threatened by the overwhelming 2-jet backgrounds. In order to get rid of those backgrounds, one can first demand high transverse energy (E_T^J) for both of the jets, as shown in the second column of Table II. In addition, one can utilize the "fatness" of the jets as a discriminator. We define a fat jet (J) with cone size

$$\Delta R_J < 0.8 \tag{26}$$

Since the two jets merged into one J in the case of the signal will have an invariant mass peaking at M_W, we further demand two such mass peaks, each within

$$m_{J_1} = m_{J_2} = M_W \pm 15 \text{ GeV}. \tag{27}$$

While all signal events show this feature, the typical jets from QCD partons would not have large mass. In reality, however, light quarks and gluons do develop parton showers due to QCD radiation and thus lead to finite mass. Some simulations show that an effective jet mass scales with its transverse energy roughly like $m_J \approx (10-15)\% E_T^J$. For a jet to acquire

Rate (fb)	Basic Cuts	$\max(E_T^J) > 200$ GeV $\min(E_T^J) > 140$ GeV	Jet mass m_J $M_W \pm 15$ GeV	M_{JJ} 600 ± 75 GeV
signal	3.62×10^{-2}	3.61×10^{-2}	3.60×10^{-2}	3.60×10^{-2}
$JJW^{\pm}W^{\pm}$	14.53	4.66	0.18	1.68×10^{-4}

TABLE II: The signal and the leading background rates for $pp \to W^+W^+W^-W^- \to JJ + \ell^+\ell^+ + \not{E}_T$. The rates after imposing each selection criterion, as described in the text, are shown. $m_{H^{++}} =$ 600 GeV. $\mu_R = \mu_F = \sqrt{s/4}$ for $JJW^{\pm}W^{\pm}$ calculation.

a mass of the order of M_W, say 65 GeV, its transverse energy would have to be at least 500 GeV. We will thus require an E_T^J on the order of 500 GeV for the background jets. The demand of such a high E_T^J suppresses the backgrounds quite effectively. The final killer of the backgrounds is the demand to reconstruct $M_{H^{++}} = m(W^+W^+) = M_{JJ}$.

We illustrate the effectiveness of these steps by explicitly evaluating a leading background $jjW^{\pm}W^{\pm}$ from QCD processes. The results are listed in Table II. Once again, the signal observation is mainly a statistical issue after the elimination of the backgrounds. As already seen in Fig. 9(b), the surviving rates persented here show that an integrated luminosity of 300 fb^{-1} should allow for extracting the signal of about 700 GeV doublly charged Higgs in this channel.

V. SUMMARY AND CONCLUSIONS

We have investigated the visibility of the pair-production of doubly charged scalars at the LHC. Such a scalar is assumed to belong to an SU(2)$_L$ triplet which can generate Majorana masses for left-handed neutrinos through the vev of its neutral component. Pair-production, in spite of its relative kinematical suppression, has the advantage of being relatively model-independent, and is not driven by the vev of the triplet. We find that, while the contribution comes largely from the Drell-Yan process, two-photon fusion also contributes at the level of 10% at the LHC due to the substantially enhanced electromagnetic coupling. This, we emphasize, is comparable to the QCD correction to the Drell-Yan channel, and must be included in a complete and accurate estimate.

Signatures of the pair-produced scalars have been investigated over the entire parameter space where viable neutrino masses can arise from the scalar triplet. We have covered both

the regions where they decay dominantly into like-sign dileptons and like-sign W's. The former are largely free from backgrounds, and a mass range upto about 800 GeV to 1 TeV can be probed with an integrated luminosity of 300 fb^{-1}, if the doubly charged Higgs has a branching ratio of at least $30\% - 60\%$ in this channel. In the latter channel, we have suggested optimal ways of eliminating the standard model backgrounds with high efficiency for the signal retention. The signal observation is mainly a statistical issue, and a doubly charged scalar of mass up to about 700 GeV should be identifiable, if it dominantly decays into a pair of like-sign W's. With the spirit of neutrino mass generation of Eq. (2) and the signal complementarity between the $\ell^+\ell^+$ and W^+W^+ channels as shown in Fig. 9(b) by the 3-event contours, we claim a complete coverage for $M_{H^{++}} \approx 650$ GeV with any arbitrary decay of these two modes.

There has been great interest of searches for long-lived doubly charged scalars. We found that in order to have the requisite contribution to neutrino masses, it is not possible for the scalar to be long-lived, although it is possible to leave a perceptible decay gap at the detector for $M_{H^{++}} \lesssim 250$ GeV. Any observation of long-lived scalars of this kind will therefore be a pointer towards some alternative theory of neutrino masses such as the Type II seesaw mechanism. Finally, we wish to emphasize that a study of the decays of the doubly charged scalar into different lepton flavors, diagonal as well as off-diagonal, is a very useful probe of the mechanism whereby neutrino masses arise from interaction with an $\mathrm{SU}(2)_L$ scalar triplet. This probe is eminently within the scope of the LHC.

Acknowledgement

We thank Patha Konar for helpful discussions. The work of TH and KW is supported in part by the U.S. Department of Energy under grant No. DE-FG02-95ER40896, by the Wisconsin Alumni Research Foundation. BM would like to thank the Department of Atomic Energy, India, for support through the Xth and XIth 5-Year Plan Projects. Si is supported by NNSFC, NCET and Huoyingdong Foundation. BM and Si would like to acknowledge the hospitality of the Phenomenology Institute, University of Wisconsin-Madison while the

work was in progress and completed.

---

[1] G. Senjanovic and R. N. Mohapatra, Phys. Rev. D **12**, 1502 (1975). R. N. Mohapatra and J. C. Pati, Phys. Rev. D **11**, 2558 (1975).

[2] H. Georgi and M. Machacek, Nucl. Phys. B **262**, 463 (1985).

[3] J. F. Gunion, J. Grifols, A. Mendez, B. Kayser and F. I. Olness, Phys. Rev. D **40**, 1546 (1989).

[4] N. Arkani-Hamed, A. G. Cohen and H. Georgi, Phys. Lett. B **513**, 232 (2001) [arXiv:hep-ph/0105239]. N. Arkani-Hamed, A. G. Cohen, E. Katz, A. E. Nelson, T. Gregoire and J. G. Wacker, JHEP **0208**, 021 (2002) [arXiv:hep-ph/0206020]. M. Schmaltz, JHEP **0408**, 056 (2004) [arXiv:hep-ph/0407143]. T. Han, H. E. Logan, B. McElrath and L. T. Wang, Phys. Rev. D **67**, 095004 (2003) [arXiv:hep-ph/0301040].

[5] D. Acosta *et al.* [CDF Collaboration], Phys. Rev. Lett. **93**, 221802 (2004) [arXiv:hep-ex/0406073].

[6] D. Acosta *et al.* [CDF Collaboration], Phys. Rev. Lett. **95**, 071801 (2005) [arXiv:hep-ex/0503004].

[7] V. M. Abazov *et al.* [D0 Collaboration], Phys. Rev. Lett. **93**, 141801 (2004) [arXiv:hep-ex/0404015].

[8] J. A. Coarasa, A. Mendez and J. Sola, Phys. Lett. B **374**, 131 (1996) [arXiv:hep-ph/9511297]. E. Ma, M. Raidal and U. Sarkar, Nucl. Phys. B **615**, 313 (2001) [arXiv:hep-ph/0012101]. P. H. Frampton, M. C. Oh and T. Yoshikawa, Phys. Rev. D **66**, 033007 (2002) [arXiv:hep-ph/0204273]. E. J. Chun, K. Y. Lee and S. C. Park, Phys. Lett. B **566**, 142 (2003) [arXiv:hep-ph/0304069].

[9] T. Han, H. E. Logan, B. Mukhopadhyaya and R. Srikanth, Phys. Rev. D **72**, 053007 (2005) [arXiv:hep-ph/0505260]. J. Y. Lee, JHEP **0506**, 060 (2005) [arXiv:hep-ph/0501118]. E. Accomando *et al.*, arXiv:hep-ph/0608079.

[10] W. M. Yao *et al.* [Particle Data Group], J. Phys. G **33**, 1 (2006).

[11] For recent review see *eg.* S.R. Elliott and J. Engel, J. Physics. **G30** R183 (2004) [arXiv:hep-ph/0405078].

[12] G. Belanger, F. Boudjema, D. London and H. Nadeau, Phys. Rev. D **53**, 6292 (1996) [arXiv:hep-ph/9508317]. D. London, arXiv:hep-ph/9907419. P. Benes, A. Faessler, F. Simkovic

and S. Kovalenko, Phys. Rev. D **71**, 077901 (2005) [arXiv:hep-ph/0501295].

[13] M. Hirsch, H. V. Klapdor-Kleingrothaus and O. Panella, Phys. Lett. B **374**, 7 (1996) [arXiv:hep-ph/9602306].

[14] C. Aalseth *et al.*, arXiv:hep-ph/0412300.

[15] J. F. Gunion, R. Vega and J. Wudka, Phys. Rev. D **43**, 2322 (1991).

[16] J. F. Gunion, R. Vega and J. Wudka, Phys. Rev. D **42**, 1673 (1990).

[17] R. S. Chivukula and H. Georgi, Phys. Lett. B **182**, 181 (1986).

[18] R. Vega and D. Dicus, Nucl. Phys. B**329**, 533 (1990)

[19] K. Huitu *et al.,* Nucl. Phys. B **487**, 27 (1997).

[20] G. Azuleos, K. Bensalma and J. Ferland, J. Phys. G32, 73 (2006).

[21] A. G. Akeroyd and M. Aoki, Phys. Rev. D **72**, 035011 (2005) [arXiv:hep-ph/0506176].

[22] M. Muhlleitner and M. Spira, Phys. Rev. D **68**, 117701 (2003) [arXiv:hep-ph/0305288].

[23] M. Drees, R. M. Godbole, M. Nowakowski and S. D. Rindani, Phys. Rev. D **50**, 2335 (1994) [arXiv:hep-ph/9403368].

[24] S. Chakrabarti, D. Choudhury, R. M. Godbole and B. Mukhopadhyaya, Phys. Lett. B **434**, 347 (1998) [arXiv:hep-ph/9804297].

[25] ATLAS TDR: CERN/LHCC/99-15.

[26] A. Hektor, M. Kadastik, M. Muntel, M. Raidal and L. Rebane, arXiv:0705.1495 [hep-ph].

[27] V. D. Barger, T. Han and H. Pi, Phys. Rev. D **41**, 824 (1990).

[28] V. D. Barger, A. L. Stange and R. J. N. Phillips, Phys. Rev. D **45**, 1484 (1992).

[29] W. Beenakker, S. Dittmaier, M. Kramer, B. Plumper, M. Spira and P. M. Zerwas, Phys. Rev. Lett. **87**, 201805 (2001) [arXiv:hep-ph/0107081]. S. Dawson, L. H. Orr, L. Reina and D. Wackeroth, Phys. Rev. D **67**, 071503(R) (2003) [arXiv:hep-ph/0211438].